Journal of the Serbian Society for Computational Mechanics / Vol. 16 / No. 1, 2022 / pp 109-124
(10.24874/jsscm.2022.16.01.08)

MIXED-MODE STRESS INTENSITY FACTOR EVALUATION BY INTERACTION INTEGRAL METHOD UNDER THERMAL AND MECHANICAL LOADS

Ait Ferhat Yazid[*1], Blaoui Mohamed Mossaab[1], Chorfi Hichem[1], Abacha Ilyes[1], Benchikh Lilia[1], Kebaili Maya[1], Boulenouar Abdelkader[2]

[1] Mechanics Research Center (CRM), BP N73B, Freres Ferrad, Ain El Bey, 25021 Constantine, Algeria
[2] Mechanical Engineering Department, Djillali Liabes University of Sidi-Bel-Abbes (22000) BP. 89, City Larbi Ben Mhidi, Algeria
e-mail: aitferhatyazid@gmail.com
**corresponding author*

Abstract

The objective of this study is to present numerical aspects related to the implementation of the interaction integral method for the purpose of determining the stress intensity factors in mode I and mixed-mode crack problems of functionally graded materials (FGM) and homogenous materials for a different form of cracking. This numerical development is based on the use of the finite element method (FEM), by the coupling of the Ansys-Matlab calculation codes. To validate the accuracy and reliability of the approach, the results obtained will be compared with other numerical results in the literature. The interaction integral method is one of the methods most compatible with the formulation of the finite element method. Therefore, we are interested in this study, in terms of the presentation of necessary steps which allow the resolution of a problem by finite elements for the mechanical problems. It is very important to note that the principle of the implementation of the "Integral M" technique is using scripts based on the coupling of two commercial software.

Keywords: Stress intensity factors, Integral M, FGM, mixed-mode, FEM.

1. Introduction

The study of material fracture is important to the notion of fracture mechanics. The fracture mechanics approach has been proven to be highly helpful in creating techniques for quality control and in-service inspection, as well as in estimating the strength of isotopic and homogenous materials in the presence of faults or cracks. Since self-similar crack formation typically does not occur in composite materials, the application of fracture mechanics to composite materials is more difficult. The most frequent type of failure in FGM is the development and progression of cracks. Therefore, it is essential to design the FGM's components and increase fracture toughness. Finding analytical solutions to complex situations is challenging since the material characteristics of FGM are a function of spatial coordinates. Various engineering issues should be resolved using numerical techniques. Within the framework of linear fracture mechanics, several numerical

methods have been proposed to evaluate the stress state in the vicinity of the crack, based on the determination of the stress intensity factors (Blackburn, 1973; Mohammed et al. 2019; Ait Ferhat and Boulenouar, 2020; Blandford et al. 1981). Among these methods is the interaction integral method which has been the subject of several studies, used to analyze the problem of cracking in mixed-mode (Yu et al. 2009; Kim and Paulino, 2003; Réthoré et al. 2005; Ammendolea et al. 2021; Feng et al. 2020).

In this study, we test the efficiency and robustness of the developed calculation program and analyze cracks in functionally graded and homogenous materials under mechanical and thermal loads. For this purpose, two examples of validation will be presented. The obtained results will be compared with other numerical works existing in the literature.

2. Theory: Formulation of the interaction integral

When the crack is stressed in mixed-mode, it becomes necessary to determine the different stress intensity factors separately. From the J integral, Yau et al. (1980) have proposed a method to determine them. This method called interaction integral is very widely used (Gosz and Moran, 2002).

We consider a mechanical state as the sum of the current state of the structure ($u^{rea}, \varepsilon^{rea}, \sigma^{rea}$) and a fictitious auxiliary state ($u^{aux}, \varepsilon^{aux}, \sigma^{aux}$). We consider two equilibrium states of the cracked body: State 1 is the real state of the studied problem satisfying the boundary conditions, and state 2 is a fictitious auxiliary state. We can then rewrite the J integral of the two states superimposed by Duflot (2004):

$$J^{(tot)} = \int_{\Gamma} \left(W^{(tot)} \delta_{1j} - (\sigma_{ij}^{(rea)} \sigma_{ij}^{(aux)}) \frac{\partial u_i^{(rea)} + u_i^{(aux)}}{\partial x_1} \right) n_j d\Gamma \tag{1}$$

where

$$W^{(tot)} = \frac{1}{2} (\sigma_{ij}^{(rea)} + \sigma_{ij}^{(aux)})(\varepsilon_{ij}^{(rea)} + \varepsilon_{ij}^{(aux)}) \tag{2}$$

Rearranging the terms, we get:

$$\begin{aligned} J^{(tot)} &= \int_{\Gamma} \left(W^{(rea)} \delta_{1j} - \sigma_{ij}^{(rea)} \frac{\partial (u_i^{(rea)})}{\partial x_1} \right) n_j d\Gamma + \int_{\Gamma} \left(W^{(aux)} \delta_{1j} - \sigma_{ij}^{(aux)} \frac{\partial (u_i^{(rea)})}{\partial x_1} \right) n_j d\Gamma \\ &+ \int_{\Gamma} \left(W^{(rea,aux)} \delta_{1j} - \sigma_{ij}^{(rea)} \frac{\partial u_i^{(aux)}}{\partial x_1} - \sigma_{ij}^{(aux)} \frac{\partial u_i^{(rea)}}{\partial x_1} \right) n_j d\Gamma \end{aligned} \tag{3}$$

$$\rightarrow J^{(tot)} = J^{(rea)} + J^{(aux)} + M^{(rea,aux)} \tag{4}$$

Where $J^{(rea)}$ $\mathrm{J}^{(\mathrm{rea})}$ and $J^{(aux)}$ $\mathrm{J}^{(\mathrm{aux})}$ are the J integrals of the current and auxiliary states, respectively. $M^{(rea,aux)}$ $\mathrm{M}^{(\mathrm{rea,aux})}$ is the interaction integral of the two states:

$$M^{(rea,aux)} = \int_{\Gamma} \left(W^{(rea,aux)} \delta_{1j} - \sigma_{ij}^{(rea)} \frac{\partial u_i^{(aux)}}{\partial x_1} - \sigma_{ij}^{(aux)} \frac{\partial u_i^{(rea)}}{\partial x_1} \right) n_j d\Gamma \tag{5}$$

Where $W^{(1,2)}$ $\mathrm{W}^{(1,2)}$ is the mutual strain energy defined by:

$$W^{(rea,aux)} = \frac{1}{2}(\sigma_{ij}^{(rea)} + \varepsilon_{ij}^{(aux)} + \sigma_{ij}^{(aux)} + \varepsilon_{ij}^{(rea)}) \tag{6}$$

It is possible to develop the expression (3) for the superposition of states, resulting in:

$$J^{(tot)} = \frac{\left(K_I^{(tot)}\right)^2}{E^*} + \frac{\left(K_{II}^{(tot)}\right)^2}{E^*} + \frac{\left(K_{III}^{(tot)}\right)^2}{2\mu} \tag{7}$$

$$\rightarrow J^{(tot)} = \frac{\left(K_I^{(rea)} + K_I^{(aux)}\right)^2}{E^*} + \frac{\left(K_{II}^{(rea)} + K_{II}^{(aux)}\right)^2}{E^*} + \frac{\left(K_{III}^{(rea)} + K_{III}^{(aux)}\right)^2}{2\mu} \tag{8}$$

$$\begin{aligned} J^{(tot)} = {} & \frac{\left(K_I^{(rea)}\right)^2}{E^*} + \frac{\left(K_{II}^{(rea)}\right)^2}{E^*} + \frac{\left(K_{III}^{(rea)}\right)^2}{2\mu} + \frac{\left(K_I^{(aux)}\right)^2}{E^*} + \frac{\left(K_{II}^{(aux)}\right)^2}{E^*} + \frac{\left(K_{III}^{(aux)}\right)^2}{2\mu} \\ & + 2\frac{K_I^{(rea)} + K_I^{(aux)}}{E^*} + 2\frac{K_{II}^{(rea)}K_{II}^{(aux)}}{E^*} + 2\frac{K_{III}^{(rea)}K_{III}^{(aux)}}{2\mu} \end{aligned} \tag{9}$$

$$\rightarrow J^{(tot)} = J^{(rea)} + J^{(aux)} + 2\left(\frac{K_I^{(rea)} + K_I^{(aux)}}{E^*} + \frac{K_{II}^{(rea)}K_{II}^{(aux)}}{E^*} + \frac{K_{III}^{(rea)}K_{III}^{(aux)}}{2\mu}\right) \tag{10}$$

μ μ is the shear modulus.

$\mathrm{E}^* = \mathrm{E}\, E^* = E$ in plane stress, and $\left(\frac{E}{1-\nu^2}\right)$ $\left(\frac{\mathrm{E}}{1\text{-}\nu^2}\right)$in plane strain.

Finally, we get:

$$M^{(rea,aux)} = 2\left(\frac{K_I^{(rea)} + K_I^{(aux)}}{E^*} + \frac{K_{II}^{(rea)}K_{II}^{(aux)}}{E^*} + \frac{K_{III}^{(rea)}K_{III}^{(aux)}}{2\mu}\right) \tag{11}$$

For a cracked two-dimensional problem$\left(K_{III}^{(rea)} = 0\right)$$(\mathrm{K}_{\mathrm{III}}^{(\mathrm{rea})} = 0)$, the expression (11) then becomes:

$$M^{(rea,aux)} = \frac{2}{E^*}\left(K_I^{(rea)}K_I^{(aux)} + K_{II}^{(rea)}K_{II}^{(aux)}\right) = M \tag{12}$$

By choosing the auxiliary fields as each of the pure modes, it is then possible to identify the value of each of the stress intensity factors. We use the following two combinations:

$$K_I{}^{(aux)} = 1.0, K_{II}{}^{(aux)} = 0.0 \rightarrow K_I{}^{(rea)} = \frac{E^*}{2}M = K_I \tag{13a}$$

$$K_{II}{}^{(aux)} = 1.0, K_{II}{}^{(aux)} = 0.0 \rightarrow K_{II}{}^{(rea)} = \frac{E^*}{2}M = K_{II} \tag{13b}$$

2.1 Evaluation of the interaction integral (Integral M)

We recall that the formulation of the Rice (1968) integral was defined as:

$$J = \int_{\Gamma} W dy - \vec{T} \frac{\partial u}{\partial x} ds \tag{14}$$

We consider a certain integral on the closed contour of Fig. 1 where the integrand is that of the integral of the equation (14) multiplied by a function q:

$$I = \int_{\Gamma} \left(W d_{1j} - \sigma_{ij} \frac{\partial u_i}{\partial x_1} \right) m_j q d\Gamma \tag{15}$$

where (m) is the normal outside the closed contour which equals (n) on Γ_2 Γ_2 and $-$ nonΓ_1 Γ_1 and δ_{1i} δ_{1i} is a Kronecher parameter.

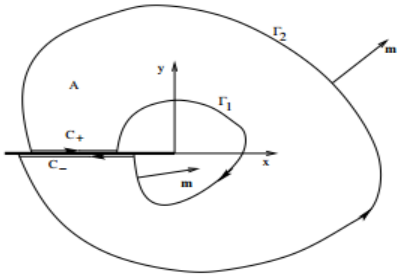

Fig. 1. Integral J.

The function qis chosen such that:

$$q = \begin{cases} 1 \rightarrow \Gamma_1 \\ 0 \rightarrow \Gamma_2 \end{cases} \tag{16}$$

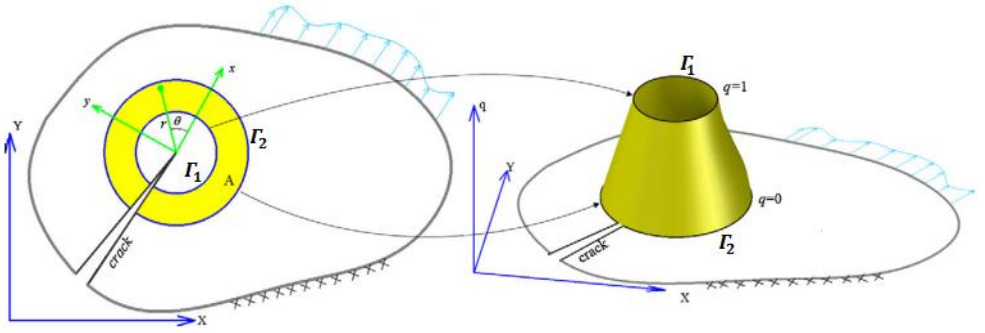

Fig. 2. Function q on the integration elements.

As q=0 on Γ_2 and that the integrand is zero on Γ_- C+and Γ_+ C-, the integral over the closed contour reduces to an integral over Γ_1 Γ_1.

$$I = \int_{\Gamma_1} \left(W d_{1j} - \sigma_{ij} \frac{\partial u_i}{\partial x_1} \right) m_j q d\Gamma = -J \tag{17}$$

By the theorem of divergence

$$I = \int_A \left[\frac{\partial}{\partial x_j} \left(W \delta_{1j} - \sigma_{ij} \frac{\partial u_i}{\partial x_1} \right) q + \left(W \delta_{1j} - \sigma_{ij} \frac{\partial u_i}{\partial x_1} \right) \frac{\partial q}{\partial xj} \right] dA \tag{18}$$

One can easily show that the first term of the equation (18) is null in linear elasticity and consequently, the form in domain of the integral J Jis:

$$I = -\int_A \left(W \delta_{1j} - \sigma_{ij} \frac{\partial u_i}{\partial x_1} \right) \frac{\partial q}{\partial xj} dA \tag{19}$$

Similarly, the interaction integral evaluated over a domain is given by Duflot (2004):

$$M^{(rea,aux)} = M = -\int_A \left(W^{(rea,aux)} \delta_{1j} - \sigma_{ij}^{\ rea} \frac{\partial u_i^{(aux)}}{\partial x_1} - \sigma_{ij}^{(aux)} \frac{\partial u_i^{(rea)}}{\partial x_1} \right) \frac{\partial q}{\partial xj} dA \tag{20}$$

3. Numerical results and discussion

3.1 The main Strategy and implementation of the method

The major objective of the current computation program is to decompose a failure mode for the purpose of extracting the SIFs K_I and K_{II} $\mathrm{K_{II}}$from the M-integral method.

From the numerical point of view, the interaction integral method is the most compatible with the formulation of the finite element method. The expression (20) defining the M-integral technique can be written in the discretized form [14-15]:

$$M = \sum_{e=1}^{e_n} \sum_{p=1}^{p_e} \left\{ \left(\sigma_{ij}^{(rea)} u_{j,1}^{(aux)} + \sigma_{ij}^{(aux)} u_{j,1}^{(rea)} - \sigma_{jk}^{(rea)} \varepsilon_{jk} \delta_{1i} \right) q_{,i} \right\} \left| Jac \right| W_p \tag{21}$$

where: e_n $\mathrm{e_n}$ is the number of elements of the integration domain A.

p_n $\mathrm{P_e}$is the number of integration points in an element, $\left|Jac\right|$ |Jac| is the determinant of the Jacobian matrix, Jac Jacand W_p $\mathrm{W_P}$are the weights of the Gaussian points.

The implementation of the resolution of the problem by the present approach (Eq.21) was done according to the following steps:

Draw two circles of origin around the crack tip, with $\mathrm{R_{11}}$ and$\mathrm{R_{22}}$. The intersection between the two surfaces represents a set of elements called Jdomain (domain A) (see Fig. 3). The contour integration is transformed to a domain integral using the function q which has been defined by the equation (16). The finite element method requires the calculation of integrals on each of the elements of the mesh. For this purpose, one makes the integration on the elements of Jdomain, by choosing the points of Gauss for each element of Jdomain (Fig. 3) with:

$$Jdomain = \left[ele_1, ele_2, ele_3, ...ele_n \right] \tag{22}$$

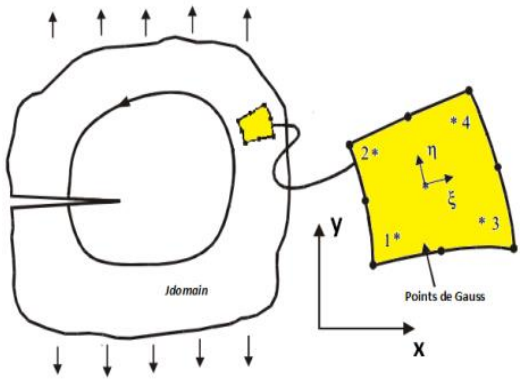

Fig. 3. Gaussian points.

1- determination of the values of the function q at each point of the Jdomain elements, q takes the value 1 inside the circle, 0 outside and values vary between 0 and 1 as shown in Fig. 4.

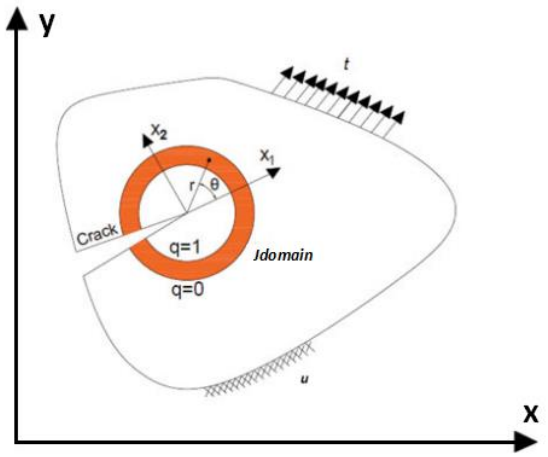

Fig. 4. Representation of the Jdomain and the function q.

2- Initialization calculation:

$M_1 = M_2 = 0, I = \begin{bmatrix} 0 & 0 \end{bmatrix}^T$ to make iterative summations.

3- for each element e of the set Jdomain, for each point of integration (ξ_i, η_i) (ξ_i, η_i), we calculate:

a) Shape functionsN_i N_i and their derivatives $\frac{\partial N_i}{\partial \xi}$ $\frac{\partial N_i}{\partial \xi}$and $\frac{\partial N_i}{\partial \eta}$ $\frac{\partial N_i}{\partial \eta}$. For the case of an isoparametric element with 4 nodes Q4 showed on Fig. 5, the functions N_i are determined by:

$$\begin{cases} N_1(\xi,\eta) = \dfrac{1}{4}(1-\xi)(1-\eta) \\ N_2(\xi,\eta) = \dfrac{1}{4}(1+\xi)(1-\eta) \\ N_3(\xi,\eta) = \dfrac{1}{4}(1+\xi)(1+\eta) \\ N_4(\xi,\eta) = \dfrac{1}{4}(1-\xi)(1+\eta) \end{cases} \tag{23}$$

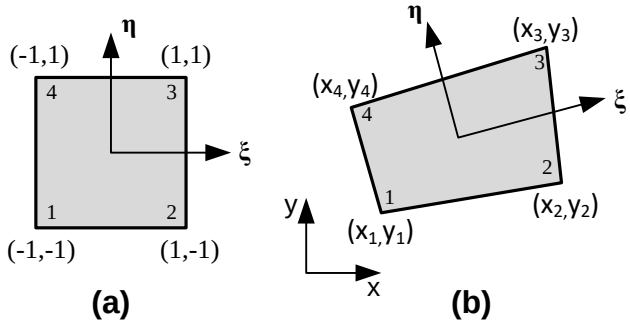

Fig. 5. Linear geometric transformation of a Q4 element: (a) The real element; (b) The deformed element.

b) The Jacobian Jac and their inverse Jac^{-1}

For each element, the Jacobian matrix is expressed as a function of the derivatives of the known geometric transformation functions and the coordinates of the geometric nodes of the real element. Indeed:

$$Jac = \begin{pmatrix} \dfrac{\partial N_1}{\partial \xi} & \dfrac{\partial N_2}{\partial \xi} & \dfrac{\partial N_3}{\partial \xi} & \dfrac{\partial N_4}{\partial \xi} \\ \dfrac{\partial N_1}{\partial \eta} & \dfrac{\partial N_2}{\partial \eta} & \dfrac{\partial N_3}{\partial \eta} & \dfrac{\partial N_4}{\partial \eta} \end{pmatrix} \begin{bmatrix} x_1 & y_1 \\ x_2 & y_2 \\ x_3 & y_3 \\ x_4 & y_4 \end{bmatrix} \tag{24}$$

$$\rightarrow Jac = \frac{1}{4}\begin{bmatrix} 1+\eta & -(1-\eta) & 1-\eta & -(1+\eta) \\ 1+\xi & -(1-\xi) & -(1+\xi) & 1-\xi \end{bmatrix} \begin{bmatrix} x_1 & y_1 \\ x_2 & y_2 \\ x_3 & y_3 \\ x_4 & y_4 \end{bmatrix} \tag{25}$$

The following transformation guarantees the transformation of the real element to the reference element:

$$\begin{Bmatrix} \frac{\partial}{\partial \xi} \\ \frac{\partial}{\partial \eta} \end{Bmatrix} = \begin{bmatrix} \frac{\partial x}{\partial \xi} & \frac{\partial y}{\partial \xi} \\ \frac{\partial x}{\partial \eta} & \frac{\partial y}{\partial \eta} \end{bmatrix} \begin{Bmatrix} \frac{\partial}{\partial x} \\ \frac{\partial}{\partial y} \end{Bmatrix} = Jac \begin{Bmatrix} \frac{\partial}{\partial x} \\ \frac{\partial}{\partial y} \end{Bmatrix} \tag{26}$$

The inverse transformation is provided by the inverse Jacobian matrix$\mathrm{Jac^{-1}}$ Jac^{-1} such that:

$$\begin{Bmatrix} \frac{\partial}{\partial x} \\ \frac{\partial}{\partial y} \end{Bmatrix} = Jac^{-1} \begin{Bmatrix} \frac{\partial}{\partial \xi} \\ \frac{\partial}{\partial \eta} \end{Bmatrix} \tag{27}$$

The inverse relation then makes it possible to calculate the first derivatives with respect to the real coordinates of the interpolation functions.

c) Determination of the values of the function q at each point of the Jdomain elements.

$$\begin{Bmatrix} \frac{\partial q}{\partial x} \\ \frac{\partial q}{\partial y} \end{Bmatrix} = Jac^{-1} \begin{Bmatrix} \frac{\partial q}{\partial \xi} \\ \frac{\partial q}{\partial \eta} \end{Bmatrix} \tag{28}$$

With

$$\begin{cases} q = 1 - \frac{\sqrt{x^2 + y^2}}{R} \\ \frac{\partial q}{\partial x} = \frac{-x}{R\sqrt{x^2 + y^2}} \\ \frac{\partial q}{\partial y} = \frac{-y}{R\sqrt{x^2 + y^2}} \end{cases} \tag{29}$$

d) Extract SIFs $K_I^{(rea)}$ $\mathrm{K_I^{(rea)}}$ and $K_{II}^{(rea)}$ $\mathrm{K_{II}^{(rea)}}$

✓ **Mode I**: we put$\mathrm{K_I^{(aux)}} = 1$ $K_I^{(aux)} = 1$, $K_{II}^{(aux)} = 0$ $\mathrm{K_{II}^{(aux)}} = 0$

3.1.1 Calculation of the auxiliary stress fields

For the two-dimensional linearized elasticity problem, in the case of an isotropic homogeneous material, the expressions of the auxiliary stress fields $\sigma_{ij}^{(aux)}$ $\mathrm{\sigma_{ij}^{(aux)}}$can be expressed by:

$$\sigma_{ij}^{(aux)} = \frac{K_I^{(aux)}}{\sqrt{2\pi r}} f_{ij}^{I}(\theta) + \frac{K_{II}^{(aux)}}{\sqrt{2\pi r}} f_{ij}^{II}(\theta) (i, j = 1,2) \tag{30}$$

where:

$\sigma_{ij}^{(aux)}$ $\sigma_{ij}^{(aux)}$ is the stress tensor, $K_I^{(aux)}$ $K_I^{(aux)}$ $K_I^{(rea)}$ and $K_{II}^{(aux)}$ $K_{II}^{(aux)}$ are the auxiliary stress intensity factors in mode I and mode II, respectively. r is the radial distance of the crack, f_{ij}^{II} f_{ij}^{II} is the function of $\theta(\theta)$ the angle of the plane of the crack.

3.1.2 Calculation of the auxiliary displacement fields

$$u_i^{(aux)} = \frac{K_I^{(aux)}}{\mu}\sqrt{\frac{r}{2\pi}}g_{ij}^{I}(\theta) + \frac{K_{II}^{(aux)}}{\mu}\sqrt{\frac{r}{2\pi}}g_i^{II}(\theta)(i=1,2) \tag{31}$$

$$\begin{cases} g_1^I(\theta) = \frac{1}{4}\left[(2k-1)\cos\frac{\theta}{2} - \cos\frac{3\theta}{2}\right] \\ g_1^{II}(\theta) = \frac{1}{4}\left[(2k+3)\sin\frac{\theta}{2} - \sin\frac{3\theta}{2}\right] \\ g_2^I(\theta) = \frac{1}{4}\left[(2k+1)\sin\frac{\theta}{2} - \sin\frac{3\theta}{2}\right] \\ g_2^{II}(\theta) = \left[(2k-3)\cos\frac{\theta}{2} + \cos\frac{3\theta}{2}\right] \end{cases} \tag{32}$$

3.1.3 Calculation of the derivations of the auxiliary displacement fields

The graduated field of auxiliary displacement $u_{i,j}^{(aux)}$ $u_{i,j}^{(aux)}$ is evaluated:

$$\begin{cases} u_{1,1}^{(aux)} = \frac{1}{8\mu\sqrt{2\pi r}}\left[K_I^{(aux)}\left((2k-1)\cos\frac{\theta}{2} + \cos\frac{5\theta}{2}\right) - K_{II}^{(aux)}\left((2k+1)\sin\frac{\theta}{2} + \sin\frac{5\theta}{2}\right)\right] \\ u_{2,1}^{(aux)} = \frac{1}{8\mu\sqrt{2\pi r}}\left[K_I^{(aux)}\left(-(2k+3)\sin\frac{\theta}{2} + \sin\frac{5\theta}{2}\right) - K_{II}^{(aux)}\left((2k-1)\cos\frac{\theta}{2} - \cos\frac{5\theta}{2}\right)\right] \\ u_{1,2}^{(aux)} = \frac{1}{8\mu\sqrt{2\pi r}}\left[K_I^{(aux)}\left((2k+1)\sin\frac{\theta}{2} + \sin\frac{5\theta}{2}\right) + K_{II}^{(aux)}\left((2k+5)\cos\frac{\theta}{2} + \cos\frac{5\theta}{2}\right)\right] \\ u_{2,2}^{(aux)} = \frac{1}{8\mu\sqrt{2\pi r}}\left[K_I^{(aux)}\left((2k-1)\cos\frac{\theta}{2} - \cos\frac{5\theta}{2}\right) + K_{II}^{(aux)}\left(-(2k-5)\sin\frac{\theta}{2} + \sin\frac{5\theta}{2}\right)\right] \end{cases} \tag{33}$$

3.1.4 Calculation of the auxiliary strain fields

The auxiliary strain fields $\varepsilon_{ij}^{(aux)}$ $\varepsilon_{ij}^{(aux)}$ can be calculated from the relations:

$$\varepsilon_{ij}^{(aux)} = \frac{1}{2}\left(u_{i,j}^{(aux)} + u_{j,i}^{(aux)}\right),(i,j=1,2) \tag{34}$$

which gives:

$$\begin{cases} \varepsilon_{11}^{(aux)} = u_{1,1}^{(aux)} \\ \varepsilon_{22}^{(aux)} = u_{2,2}^{(aux)} \\ \varepsilon_{12}^{(aux)} = \dfrac{1}{2}\left(u_{1,2}^{(aux)} + u_{2,1}^{(aux)}\right) \\ \varepsilon_{21}^{(aux)} = \varepsilon_{12}^{(aux)} \end{cases} \tag{35}$$

3.1.5 Calculation of strain energy

The mutual strain energy $W^{(rea,aux)}$ $\mathrm{W}^{(\mathrm{rea,aux})}$ is defined by:

$$W^{(rea,aux)} = \frac{1}{2}(\sigma_{ij}^{(rea)}\varepsilon_{ij}^{(aux)} + \sigma_{ij}^{(aux)}\varepsilon_{ij}^{(rea)}), (i, j = 1, 2) \tag{36}$$

The stresses $\sigma_{ij}^{(rea)}$ $\sigma_{\mathrm{ij}}^{(\mathrm{rea})}$ and the strains $\varepsilon_{ij}^{(rea)}$ are connected between them by:

In plane stress:

$$\begin{Bmatrix} \sigma_{11} \\ \sigma_{22} \\ \tau_{12} \end{Bmatrix}^{rea} = \frac{E}{(1+\nu)(1-2\nu)} \begin{bmatrix} 1-\nu & -\nu & 0 \\ -\nu & 1-\nu & 0 \\ 0 & 0 & \dfrac{(1-2\nu)}{2} \end{bmatrix} \begin{Bmatrix} \varepsilon_{11} \\ \varepsilon_{22} \\ \gamma_{12} \end{Bmatrix}^{rea} \tag{37}$$

In plane strain:

$$\begin{Bmatrix} \sigma_{11} \\ \sigma_{22} \\ \tau_{12} \end{Bmatrix}^{rea} = \frac{E}{1-\nu^2} \begin{bmatrix} 1 & \nu & 0 \\ \nu & 1 & 0 \\ 0 & 0 & \dfrac{(1-\nu)}{2} \end{bmatrix} \begin{Bmatrix} \varepsilon_{11} \\ \varepsilon_{22} \\ \gamma_{12} \end{Bmatrix}^{rea} \tag{38}$$

Calculation of the interaction integral M: we calculate the integral M by iterative summation:

$$M = \sum_{e=1}^{e_n} \sum_{p=1}^{p_e} \left\{ \left(\sigma_{ij}^{(rea)} u_{j,1}^{(aux)} + \sigma_{ij}^{(aux)} u_{j,1}^{(rea)} - \sigma_{jk}^{(rea)} \varepsilon_{jk} \delta_{1i} \right) q_{,i} \right\} \left| Jac \right| W_p \tag{39}$$

- ✓ **Mode II**: we pose: $\mathrm{K}_{\mathrm{II}}^{(\mathrm{aux})} = 1$ $K_{II}^{(aux)} = 1$, $K_I^{(aux)} = 0$ $\mathrm{K}_{\mathrm{I}}^{(\mathrm{aux})} = 0$

For this mode, we redo the same steps as those used for mode I in order to calculate the interaction integral M.

After having calculated the interaction integral M for the two failure modes, the SIFs, $K_I^{(rea)}$ $\mathrm{K}_{\mathrm{I}}^{(\mathrm{rea})}$ and $K_{II}^{(rea)}$ $\mathrm{K}_{\mathrm{II}}^{(\mathrm{rea})}$ are then determined by the relations:

$$K_I^{(rea)} = K_I = \frac{E^*}{2} M \tag{40}$$

$$K_{II}^{(rea)} = K_{II} = \frac{E^*}{2} M \tag{41}$$

In the case of FGM materials, the calculated Young's modulus $E^* = E_{tip}$ $E^* = E_{tip}$ in plane stress, and $E^* = \left(\frac{E_{tip}}{1-\nu^2}\right)$ in plane strain, E_{tip} E_{tip} is calculated at the crack tip, and both thermal and mechanical loads have been considered to investigate crack interaction effect.

3.2 Examples

3.2.1 A curved crack in homogeneous plate

Consider a thin plate with a curving crack. The plate's dimensions are L= 210 units and W= 70 units (Fig. 6. (a)) made up of only one material. In this analysis, we considered young's modulus E= 2.3 GPa and Poisson's ratio υ=0,36 as material plate properties of a polycarbonate (PSM-1), with the curving crack having a varied angle 2α and constant radius R. Perpendicular to the curved crack, this structure was loaded under a constant uniaxial tensile stress.

The numerical model carried out by using finite element calculation code has allowed us to determine the stress intensity factors from the displacement field. The solution of the problem has been calculated using 4 node quadratic elements in plane stress. The global mesh model of the plate is presented in Fig. 6. (b).

For the purpose of verifying the independence of the integration contours on the evaluation of SIFs by the global approach, different domains are created from the contours surrounding the crack tip. Each contour encompasses the previously defined contour to which we add elements directly in contact with it. The integral interaction M was calculated through 03 domains (with R_1=1 units, R_2=2 units, R_3= 3 units, R_4= 4 units), as shown in Fig. 6. (c).

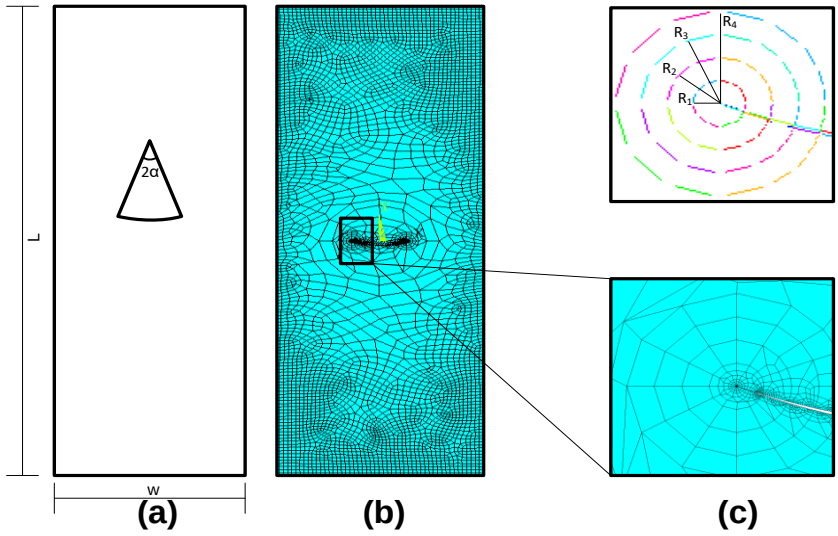

Fig. 6. (a) Dimensions of plate; (b) The global mesh of the plate with curved crack; (c) The detailed mesh and the areas of integration around the crack tip.

For this problem, the reference solutions for the stress intensity factor provided by Kablia et al. (2017) and Gdoutos (2005) are compared with our solution evaluated by the M-integral method.

$$K_I = \frac{\sigma}{2}\sqrt{R\sin\alpha}\left[\frac{\left(1-\sin^2\frac{\alpha}{2}\cos^2\frac{\alpha}{2}\right)\cos\frac{\alpha}{2}}{1+\sin^2\frac{\alpha}{2}}+\cos\frac{3\alpha}{2}\right] \tag{42}$$

$$K_{II} = \frac{\sigma}{2}\sqrt{R\sin\alpha}\left[\frac{\left(1-\sin^2\frac{\beta}{2}\cos^2\frac{\beta\alpha}{2}\right)\sin\frac{\alpha}{2}}{1+\sin^2\frac{\alpha}{2}}+\sin\frac{3\alpha}{2}\right] \tag{43}$$

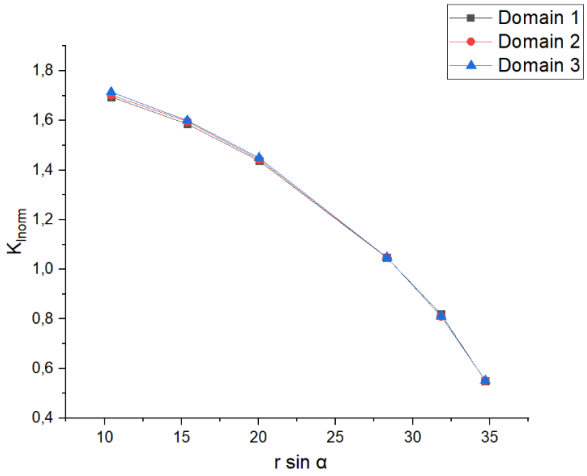

Fig. 7. Variation of normalized SIF in mode I: Independent of integration domain.

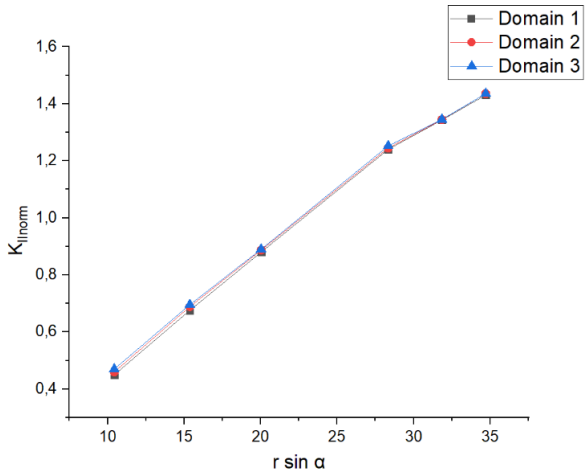

Fig. 8. Variation of normalized SIF in mode II: Independent of integration domain.

It is clearly seen in Figs 7 and 8 that the values of the normalized SIF in mode I and mode II are independent of the domain chosen. The calculation by this approach can also be performed far from the crack tip and its singularity.

The results of the present study (M-integral), the numerical study by Kablia et al. (2017) and the analytical study by Gdoutos (2005) which show the stress intensity factors for the plate containing a curved crack subjected to traction in mode I, are given in Fig. 9, and for mode II in Fig. 10, where:

$$K_{Inorm} = \frac{K_I}{\sigma\sqrt{r\sin\alpha}} \tag{44}$$

$$K_{IInorm} = \frac{K_{II}}{\sigma\sqrt{r\sin\alpha}} \tag{45}$$

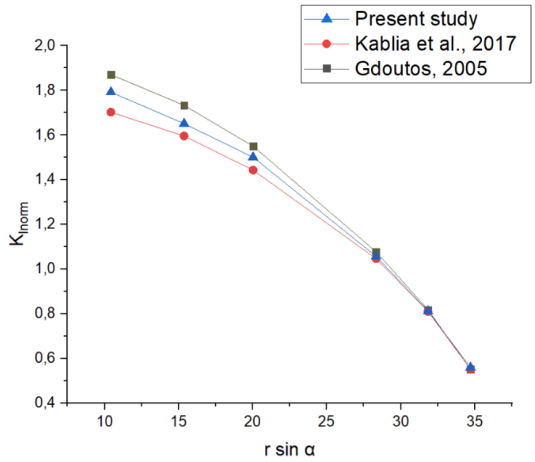

Fig. 9. Evolution of the normalized stress intensity factors in mode I according to the opening crack angle.

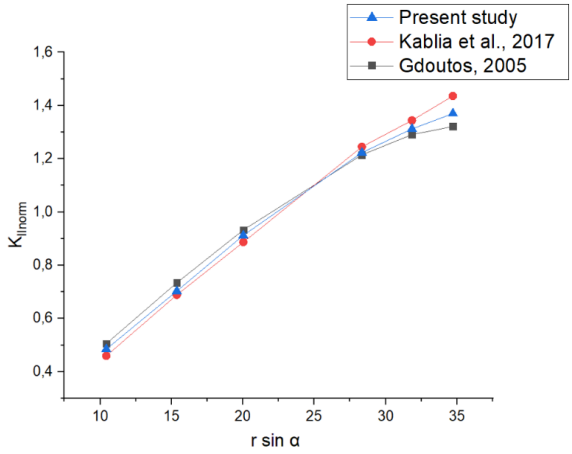

Fig. 10. Evolution of the normalized stress intensity factors in mode II according to the opening crack angle.

The comparative study has shown that the results obtained by our M-integral method are in good agreement with those obtained by the finite element method by Kablia et al. (2017) and the analytical method by Gdoutos (2005). This comparison allows us to conclude that the technique used, adequately describes the stress field in the vicinity of the crack tip.

3.2.2 A thermally stressed hollow cylinder with two radial side cracks

In this first example, an infinite hollow cylinder with two radial edge cracks is examined. The internal surface of the hollow cylinder is where the cracks are located. A permanent temperature gradient is prescribed with temperature T_1= 30° on the internal surface R_1= 80 units and T_2= 200° on the external surface R_2= 100 units. Because of the symmetry, only a half of the cross section is analyzed with the boundary conditions shown in Fig.11. (a). To test the computer code, we have selected homogeneous isotropic material properties: E= 7.8×10^{-1} GPa, ν = 0.3 and thermal expansion coefficient α=$0.125\times10^{-4}\,\theta^{-1}\,\theta^{-1}$. The structure considered is meshed by quadratic elements, and particularly, special elements were used to characterize the singularity around the crack tip (Fig. 11. (b)), and the crack length is indicated in (a). The normalized stress intensity factor is defined as:

$$f_I = \frac{K_I}{\sqrt{\pi a}} \frac{1-\nu}{(\theta_2 - \theta_1)\alpha E} \tag{46}$$

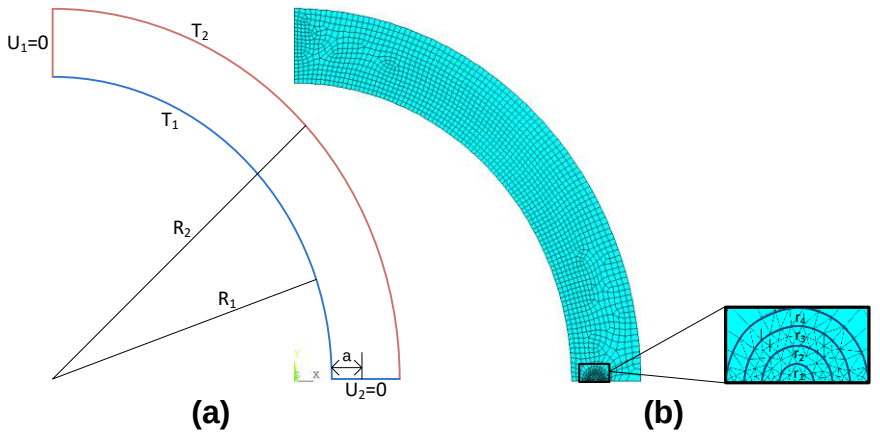

Fig. 11. (a) Hollow cylinder with boundary conditions; (b) Global and detail FE mesh for hollow cylinder.

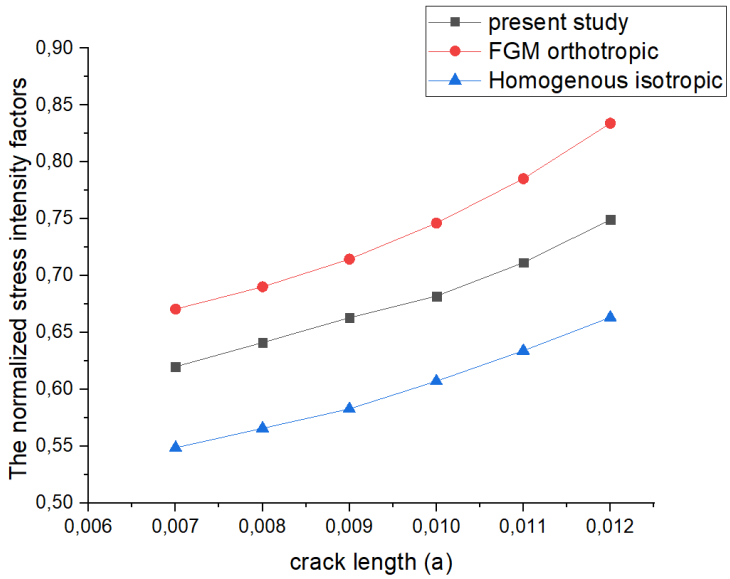

Fig. 12. The numerical results for variation of the normalized SIF with the crack length.

Variation of the normalized SIF with the crack length is presented in Fig. 12. One can observe that SIF increases with increasing the length of cracks. This comparison indicates good agreement between the results obtained in mode I. The numerical procedure thus gives a very satisfactory result, in the case of the cracks located at the material gradation.

4. Conclusions

The main objective of this paper is to present the principle of the implementation of the domain integral method in FGM and homogenous materials, in order to determine the SIF in different modes. This numerical development is based on the use of the method element finite, by a combined calculation between software Ansys and Matlab.

For the purpose of verifying the independence of the integration contours on the evaluation of the SIFs by the global approach, different domains are created from the contours surrounding the crack tip.

Mode I and mixed-mode crack problems of FGM and homogenous materials are presented. It was found that all the SIFs computed by the presented formulations are equally accurate.

The results show the variation of the SIF values depending on crack sizes (a). It can be clearly seen that the values of the SIF are independent of the chosen domain.

The link between Matlab and software dedicated to finite element calculations such as Ansys will make it possible to obtain more precise results. Moreover, with this interaction, problems with more complex geometries can be handled. The calculation by this approach can also be carried out far from the crack tip and its singularity, which makes the calculation more precise.

The good performance of the developed program has been clearly demonstrated and validated, by numerical and analytical approaches, through sufficiently varied examples of applications.

References

Ammendolea D, Greco F, Lonetti P, Luciano R, Pascuzzo A (2021). Crack propagation modeling in functionally graded materials using Moving Mesh technique and interaction integral approach. *Composite Structures*, *269*, 114005.

Ait Ferhat Y, Boulenouar A. (2020). Computation of SIFs for cracks in FGMs and TBC under mechanical and thermal loadings. *International Journal on Interactive Design and Manufacturing (IJIDeM)*, *14*(4), 1347-1356.

Benmessaoud A (2012). Contribution à la modélisation dynamique des structures fissurées soumises à des sollicitations sismiques par la méthode des éléments finis étendue (X-FEM), Memory of Magister, University of Djelfa (Algeria).

Blackburn WS (1973). Calculation of stress intensity factors at crack tips using special finite elements. In *The mathematics of finite elements and applications* (pp. 327-336). Academic Press.

Blandford GE, Ingraffea AR, Liggett JA (1981). Two-dimensional stress intensity factor computations using the boundary element method. *International Journal for Numerical Methods in Engineering*, *17*(3), 387-404.

Duflot M (2004). Application des méthodes sans maillage en mécanique de la rupture, Doctoral thesis in applied sciences, University of Liège.

Feng WZ, Gao LF, Dai YW, Qian W (2020). DBEM computation of T-stress and mixed-mode SIFs using interaction integral technique. *Theoretical and Applied Fracture Mechanics*, *110*, 102795.

Gdoutos EE (2005). Fracture Mechanics an introduction", *Solid Mechanics and its application*.second edition,

Gosz M, Moran B (2002). An interaction energy integral method for computation of mixed-mode stress intensity factors along non-planar crack fronts in three dimensions. *Engineering Fracture Mechanics*, 69(3), 299-319.

Hon Y, Wu L, Guo L, He Q, Du S (2010). Interaction integral method for the interfacial fracture problems of two nonhomogeneous materials. *Mechanics of Materials*, *42*(4), 435-450.

Kablia A, Tamine T, Hadj-meliani M, Azari Z (2017). Determination of stress intensity factors for a bi-material ring spicemen with curved cracks under compressive loading. *A- Sciences fondamentales et Engineering*, *16*, 56-62

Kim JH and Paulino GH (2003). T-stress, mixed-mode stress intensity factors, and crack initiation angles in functionally graded materials: a unified approach using the interaction integral method. *Computer methods in applied mechanics and engineering*, *192*(11-12), 1463-1494.

Mohammed O, Kareem AK, Jamian S, Nemah MN (2019). Distribution of mode I stress intensity factors for single circumferential semi-elliptical crack in thick cylinder. *International Journal of Integrated Engineering*, *11*(7), 102-111.

Réthoré J, Gravouil A, Morestin F, Combescure A (2005). Estimation of mixed-mode stress intensity factors using digital image correlation and an interaction integral. *International Journal of Fracture*, *132*(1), 65-79.

Rice J (1968). A Path Independent Integral and the Approximate Analysis of Strain Concentration by Notches and Cracks. *Journal of Applied Mechanics*, *35*(2), 379.

Yau J F, Wang SS. and Corten HT (1980). A mixed-mode crack analysis of isotropic solids using conservation laws of elasticity. *Journal of Applied Mechanics*, 47, 335–341.

Yu H, Wu L, Guo L, Du S, He Q (2009). Investigation of mixed-mode stress intensity factors for nonhomogeneous materials using an interaction integral method. *International Journal of Solids and Structures*, *46*(20), 3710-3724.